J. Fluid Mech. (2026), *vol.* 1032, A10, doi:10.1017/jfm.2026.11349

JFM PAPERS

Onset of spiral vortex breakdown in supersonic flows

Toshihiko Hiejima

Department of Aerospace Engineering, Osaka Metropolitan University, 1-1 Gakuen-cho, Nakaku, Sakai, Osaka 599-8531, Japan

Corresponding author: Toshihiko Hiejima, hiejima@omu.ac.jp

(Received 29 July 2025; revised 4 February 2026; accepted 15 February 2026)

The onset of vortex breakdown in supersonic flows remains an unsolved problem in physics. In this study, a sufficient condition for spiral vortex breakdown to occur in supersonic flows was derived from the conserved total enthalpy at the vortex axis under complete supersonic inflow conditions. The theoretical threshold was simply determined by the relationship between the magnitudes of the kinetic and internal energies (i.e. axial velocity squared and static temperature, respectively) downstream. In addition, it was found that the squared velocity and static temperature in the sufficient condition were closely related to a rapid reduction in the helicity, which indicated that vortex breakdown occurred. Numerical simulations confirmed that the theoretical threshold corresponds to the onset of spiral vortex breakdowns in supersonic flows.

Key words: vortex breakdown, supersonic flow, vortex instability

1. Introduction

Spaceplanes use delta wings to take advantage of the characteristics of supersonic flows. Several decades ago, the vortex breakdown phenomenon was discovered, wherein vortices flowing over delta wings (Peckham & Atkinson 1957; Lambourne & Bryer 1961) and in pipes (Sarpkaya 1971) suddenly burst. It has been reported that the transition point of vortex breakdown over a delta wing moves upstream as the Reynolds number increases (Van Dyke 1982). Vortex breakdowns can be defined as an abrupt change in the vortex structure of an axial flow and has strongly nonlinear characteristics, which can include a sudden increase in the size of the vortex core, a large adverse pressure gradient, the appearance of a free stagnation point near the axis, the formation of a reversed flow and a highly unstable structure (Hall 1972; Leibovich 1978; Escudier 1988; Delery 1994;

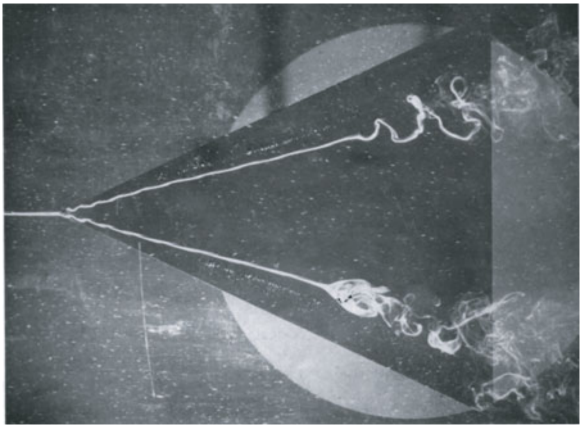

Figure 1. Photograph of a spiral-type (top side) and bubble-type (bottom side) vortex breakdown observed over a delta wing (photo taken from Lambourne & Bryer (1961)).

Lucca-Negro & O'Doherty 2001). Although some studies considered a stagnation point to be necessary for vortex breakdown to occur (Leibovich 1978), other studies showed that the stagnation point disappears at high Reynolds numbers (Novak & Sarpkaya 2000). Therefore, no clear consensus on the presence of a stagnation point has yet been established.

Vortex breakdowns have two principal configurations (figure 1): the bubble-type breakdown is almost axisymmetric in shape while the spiral-type breakdown is highly asymmetric in shape. Bubble vortex breakdowns have been observed to transition to spiral vortex breakdowns (Althaus *et al.* 1995; Ruith *et al.* 2003). A spiral vortex breakdown is regarded as a nonlinear global mode that is caused by the appearance of a locally absolute unstable region in the wake of a bubble vortex breakdown (Gallaire *et al.* 2006).

At present, there is no generally accepted theory on vortex breakdowns. However, for incompressible flows, the onset of vortex breakdown was found to be governed by the swirl strength (i.e. critical swirl number) (Spall, Gatski & Grosch 1987). A vortex breakdown in an incompressible flow is characterised by a change in the sign of the azimuthal vorticity near the axis, which is obtained from the momentum equation (Brown & Lopez 1990). The abrupt change in structure means that a vortex breakdown cannot be explained by hydrodynamic instability and instead suggests the existence of a critical state (i.e. transition from a supercritical flow state to a subcritical flow state) like that observed for hydraulic jumps and shock waves (Benjamin 1962). Ultimately, a vortex breakdown appears to comprise a transition between two conjugate flow states (Escudier 1988; Hall 1972; Leibovich 1978; Keller 1994).

While many studies have investigated vortex breakdowns in incompressible flows, only a few have investigated vortex breakdowns in shock-free compressible flows (Mahesh 1996; Rusak & Lee 2002; Hiejima 2017). For supersonic flows, some studies have investigated vortex breakdown due to the interaction between streamwise vortices and shock waves (Kalkhoran & Smart 2000), which produces a structure similar to the structure of the bubble-type vortex breakdown in incompressible flows (Delery 1994; Kalkhoran & Smart 2000; Hiejima 2014, 2023; Iwabayashi *et al.* 2024). In shock-free supersonic flows, only spiral vortex breakdowns have been reported with axial acceleration (Hiejima 2018). The vortex breakdown structure is very similar to the structure of the spiral-type vortex breakdown without stagnation points for incompressible flows at high Reynolds numbers (Novak & Sarpkaya 2000). (A stagnation point may not be required for spiral vortex

https://doi.org/10.1017/jfm.2026.11349 Published online by Cambridge University Press

breakdown, except for low Reynolds numbers.) An onset condition for vortex breakdown derived from the axial momentum variation was proposed in a previous study (Hiejima 2018). Supersonic vortex breakdown occurs when the swirl number and Mach number are small. Furthermore, bubble-type vortex breakdowns with a stagnation point occurring in subsonic flow regions cannot occur at supersonic flow conditions. Note that the derivation of the onset condition is based on the incompressible critical swirl number. Therefore, the onset mechanism for a vortex breakdown to occur in a compressible flow still needs to be identified, especially for shock-free flows. Understanding vortex breakdown in supersonic flows remains an unsolved problem in physics.

Since there are many elements associated with the onset of vortex breakdown (Lucca-Negro & O'Doherty 2001), theoretically determining a dominant condition necessary for a vortex breakdown to occur is difficult. In contrast, the concept of two conjugate flow states can be used to describe a sufficient condition for a vortex breakdown to feasibly occur regardless of the difference between incompressible and compressible flows, which can be defined as a subcritical state after the transition. In this study, a sufficient condition is described for spiral vortex breakdown to occur in a shock-free supersonic flow based on the energy conserved along the vortex axis. The theoretical threshold was verified in three-dimensional (3-D) direct numerical simulations.

2. Conditions for vortex breakdown in supersonic flows

This study used the dimensionless physical variables described in a previous study (Hiejima 2017), where u_i is the velocity vector, ρ is the density, p is the pressure and T is the temperature. The nondimensionalised state equation is $p = \rho T$. Let us assume that at high Reynolds numbers in shock-free supersonic flows with a steady and axisymmetric vortex, the field exhibits an adiabatic flow. Then, the total enthalpy $\mathscr{H}_t$ is expressed as the sum of the kinetic and internal energies (Anderson 2003):

$$\mathscr{H}_t = \frac{1}{2}u_k u_k + \int \frac{\mathrm{d}p}{\rho} = \frac{1}{2}u_k u_k + \frac{\gamma}{\gamma-1}\frac{p}{\rho} = \frac{1}{2}u_k u_k + \frac{\gamma}{\gamma-1}T, \tag{2.1}$$

where γ is the ratio of specific heats and a constant. Differentiating (2.1) with respect to x gives

$$\frac{\partial \mathscr{H}_t}{\partial x} = \frac{1}{2}\frac{\partial (u_k u_k)}{\partial x} + \frac{\gamma}{\gamma-1}\frac{\partial T}{\partial x}. \tag{2.2}$$

Note that $u_i = (u, v, w)$ in Cartesian coordinates.

To better understand the vortex breakdown conditions, the distinctive physical variables at the vortex axis (i.e. x-axis) should be considered. Suppose that v and w regarding radial transport are negligible near the axis. The occurrence of vortex breakdown is characterised by a notable change in the axial momentum J (Benjamin 1962; Mager 1972; Brown & Lopez 1990), which is defined as

$$J = \rho u^2 + p = \rho \left(u^2 + T\right). \tag{2.3}$$

For bubble vortex breakdown in a supersonic flow caused by interactions with shock waves, the deceleration of the flow due to the vortex breakdown ($\partial u/\partial x < 0$) and the appearance of a stagnation point result in the following expressions (Delery 1994; Wei *et al.* 2022; Hiejima 2023):

$$\frac{\partial u^2}{\partial x} < 0, \quad \frac{\partial J}{\partial x} < 0. \tag{2.4}$$

For spiral vortex breakdown in a supersonic flow, the acceleration of the flow due to the vortex breakdown ($u > 0$ and $\partial u/\partial x > 0$) results in the following expressions (Hiejima 2017, 2018):

$$\frac{\partial u^2}{\partial x} > 0, \quad \frac{\partial J}{\partial x} > 0. \tag{2.5}$$

The derivative of J/ρ with respect to x is given by

$$\frac{\partial}{\partial x}\left(\frac{J}{\rho}\right) = \frac{\partial u^2}{\partial x} + \frac{\partial T}{\partial x}. \tag{2.6}$$

As $\mathscr{H}_t$ is conserved in an adiabatic flow under the inviscid condition, $\partial \mathscr{H}_t/\partial x = 0$. Then, (2.2) and (2.6) can be used to obtain

$$\frac{\partial}{\partial x}\left(\frac{J}{\rho}\right) = -\frac{\gamma+1}{\gamma-1}\frac{\partial T}{\partial x}. \tag{2.7}$$

For bubble vortex breakdown, (2.4) and (2.7) indicate that the condition for its onset is given by

$$\frac{\partial T}{\partial x} > 0 \quad \text{or} \quad -\frac{\partial p}{\partial x} < 0. \tag{2.8}$$

Note that this ensures a subsonic state regarded as incompressible flow near the stagnation point. It follows that an adverse pressure gradient is essential for bubble vortex breakdown. For spiral vortex breakdown, (2.6) is transformed into

$$\frac{\partial J}{\partial x} = \rho\frac{\partial}{\partial x}\left(\frac{J}{\rho}\right) + \frac{J}{\rho}\frac{\partial \rho}{\partial x}. \tag{2.9}$$

It is reasonable to suppose that the flow field is in a stationary state. Based on the mass conservation equation, the following relation can be obtained:

$$\frac{\partial \rho}{\partial x} \approx -\frac{\rho}{u}\frac{\partial u}{\partial x}. \tag{2.10}$$

Substituting (2.7) and (2.10) into (2.9) gives

$$\frac{\partial J}{\partial x} = -\frac{\gamma+1}{\gamma-1}\rho\frac{\partial T}{\partial x} - \frac{J}{u}\frac{\partial u}{\partial x}. \tag{2.11}$$

Then, applying $\partial u/\partial x > 0$ and $\partial J/\partial x > 0$ in (2.5) to (2.11) gives the following condition:

$$\frac{\partial T}{\partial x} < 0. \tag{2.12}$$

Based on the above-mentioned relations, figure 2 shows the schematics of the temperature and squared velocity profiles of vortex breakdown at the centreline of a supersonic flow. For bubble vortex breakdown, the condition for its onset is obtained from the stagnation point $u_i = 0$ (strong constraint) (Hiejima 2023). The condition for the onset of spiral vortex breakdown can be obtained by combining the conservation of total enthalpy in (2.1) and the inequality in (2.12):

$$\frac{1}{2}u_2^2 > \frac{\gamma}{\gamma-1}T_2, \tag{2.13}$$

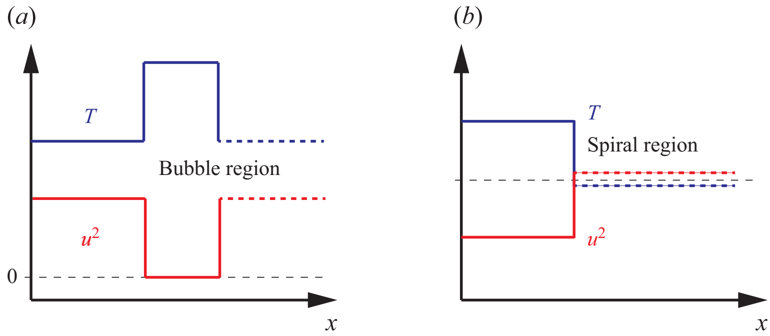

Figure 2. Schematics of temperature T and squared velocity u^2 profiles at the centreline of a supersonic flow for (a) bubble and (b) spiral vortex breakdown.

where subscripts 1 and 2 denote upstream and downstream, respectively, of the point at which the breakdown occurred. This expression is equivalent to

$$M_2 > \sqrt{\frac{2}{\gamma - 1}}, \tag{2.14}$$

where M_2 denotes the local Mach number. From a momentum perspective, the following expression can be obtained from (2.3) and (2.13):

$$\frac{J_2}{\rho_2} = u_2^2 + T_2 > \frac{3\gamma - 1}{\gamma - 1} T_2. \tag{2.15}$$

From $p_2 = \rho_2 T_2$, (2.15) can be rewritten as

$$\frac{J_2}{p_2} > \frac{3\gamma - 1}{\gamma - 1}. \tag{2.16}$$

Based on (2.14) and (2.16), the two thresholds α^* and β^* can be defined as follows:

$$\alpha^* = \frac{M_2}{\sqrt{\dfrac{2}{\gamma - 1}}} > 1, \quad \beta^* = \frac{\left(\dfrac{J_2}{p_2}\right)}{\left(\dfrac{3\gamma - 1}{\gamma - 1}\right)} > 1. \tag{2.17}$$

Therefore, the sufficient condition for a spiral vortex breakdown can be estimated by using the inequalities in (2.17).

3. Helicity density equation

The helicity density h is related to vortex breakdowns in that qualitative changes in the flow topology arising from a vortex breakdown are linked to large changes in helicity (Moffatt & Tsinober 1992). Many studies have demonstrated that the change in helicity is an important indicator that a vortex breakdown occurred (Spall & Gatski 1990; Hiejima 2018, 2020; Sharma & Sameen 2020). According to Darmofal (1994), a vortex breakdown can be regarded as an inviscid transition in incompressible flows at Reynolds numbers above 300. The inviscid helicity density equation (Boutros & Gibbon 2025) is given by

$$\frac{\partial h}{\partial t} + \frac{\partial}{\partial x_i}\left[h u_i + \omega_i \left(\frac{p}{\rho} - \frac{1}{2} u_k u_k\right)\right] = 0, \tag{3.1}$$

where $h(=u_k\,\omega_k)$ is the helicity density and ω_i is the vorticity vector. Equation (3.1) indicates that $T(=p/\rho)$ and $u^2/2$ contribute to the development of h, which represents the vortex core.

4. Velocity profiles in vortex flows

Flows with a vortex structure are assumed to be steady and axisymmetric upstream. To study vortex breakdown in supersonic flows, the vortex flow was assumed to be a Batchelor vortex (Batchelor 1964) because the velocity profile is compatible with experimental measurements of supersonic flows at high Reynolds numbers (Cattafesta & Settles 1992; Hiejima 2019). In cylindrical coordinates, the nondimensionalised velocities of a Batchelor vortex are given by

$$u_r(r) = 0, \quad u_\theta(r) = M_1 \frac{q}{r}\left(1 - e^{-r^2}\right), \quad u_x(r) = M_1\left(1 - \mu\, e^{-r^2}\right), \tag{4.1}$$

where q is the swirl intensity (circulation), μ is the axial velocity deficit and M_1 is the upstream Mach number. Because the flow does not appreciably depend on the viscosity at high Reynolds numbers, the density and pressure required for compressible flows are determined by assuming that the total enthalpy is uniform (Hiejima 2017).

5. Results and discussion

In this study, spiral vortex breakdown is investigated because bubble vortex breakdown does not occur in shock-free supersonic flows. To verify that (2.17) represents the sufficient condition for spiral vortex breakdown, numerical simulations were conducted using the 3-D unsteady compressible Navier–Stokes equations. Supersonic vortex flows expressed in (4.1) were used with four cases of q and $\mu = 0.5$ at $M_1 = 2.5$, 3.5 and 5.0, and $Re = 9000$. Further details on the methodology and conditions are stated in a previous study (Hiejima 2017) except for $0 \leqslant x \leqslant 400$.

Figure 3 shows the vortex structures of a shock-free supersonic flow using the isosurface of the second invariant of the velocity gradient tensor for visualisation (Jeong & Hussain 1995) at $M_1 = 2.5$ and 3.5. The results show that q clearly affects the evolution of a vortex. When $q \leqslant 0.08$, vortex breakdown with large spiral structures is observed. When $q = 0.24$, weak spiral structures appear after the transition, exhibiting a small outward extension in the radial direction. However, when $q = 0.16$, the structure of the observed vortex is intermediate of the two previous structures. Therefore, it is difficult to discriminate between structures with and without vortex breakdown.

Figures 4 and 5 show the different physical values at the centreline with and without vortex breakdown, respectively. When vortex breakdown occurs, the squared velocity u^2 increases rapidly and the static temperature T decreases significantly (figures 4*a* and 5*a*). It is important for these profiles to satisfy (2.13) that the kinetic energy exceeds the internal energy at the centreline. The plots indicate that the jump condition in the vortex breakdown (Benjamin 1962; Escudier 1988; Keller 1994) is intrinsically correct. The results can also be explained as follows. With vortex breakdown, u and ρ increase downstream (Hiejima 2017), so that $u^2/2 > \gamma\, T/(\gamma - 1) = [\gamma\,/(\gamma - 1)](p/\rho)$ is also necessarily satisfied; this means an increase in a component of the momentum ρu^2. The occurrence of vortex breakdown is characterised by a notable change in the momentum flux $J = \rho u^2 + p$. In supersonic vortex breakdown, an increase in ρu^2 causes a rapid increase in the momentum, instead of an increase in pressure p, which is the main cause of incompressible vortex breakdown and is also caused by downstream obstacles. Without vortex breakdown, $u^2/2 < \gamma\, T/(\gamma - 1)$ is satisfied downstream (figures 4*b* and

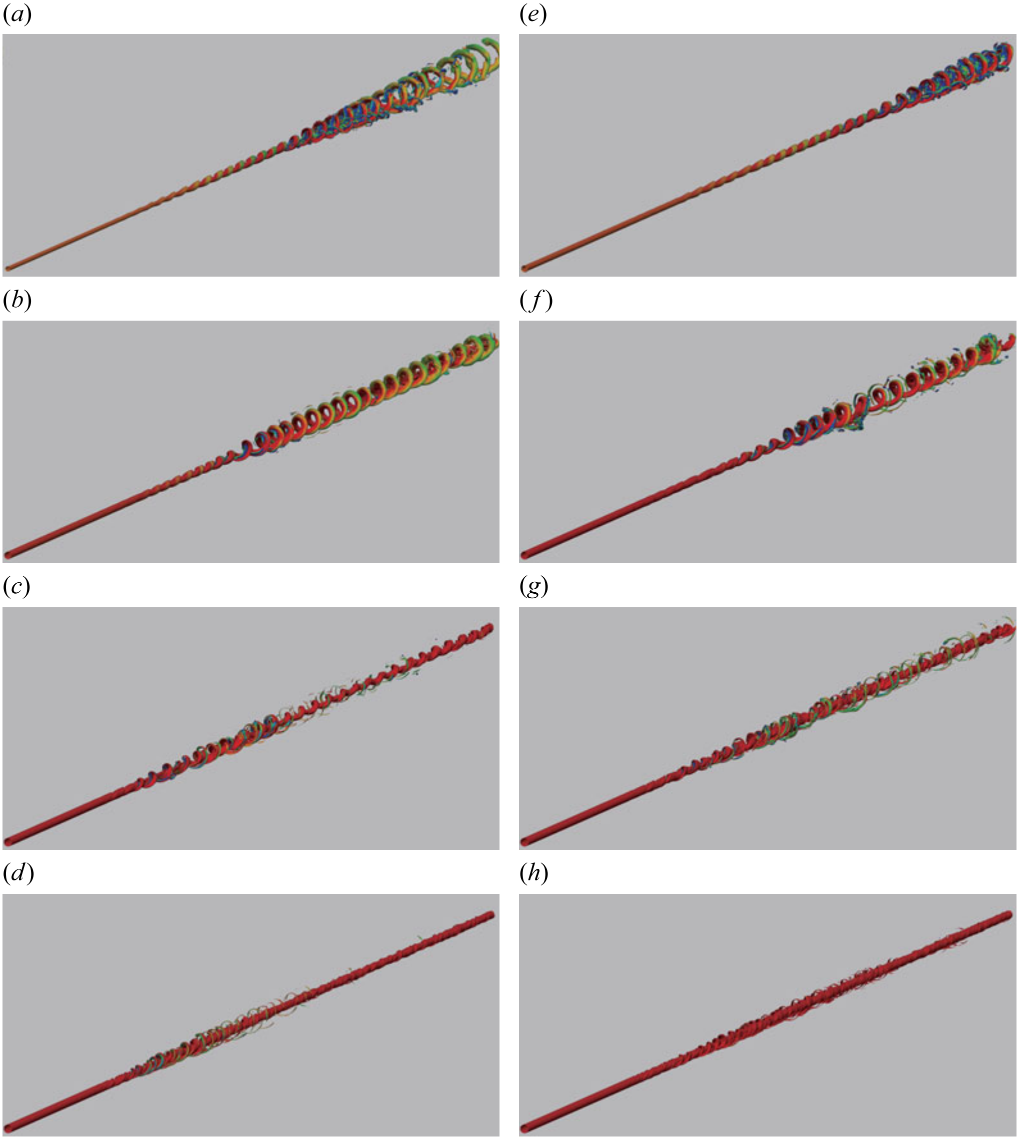

Figure 3. Vortex structures in a supersonic flow ($\mu = 0.5$) visualised using the isosurface of the second invariant of the velocity gradient tensor $\mathcal{Q}$ and colour-rendered according to the axial vorticity ω_x at: (*a*) $M_1 = 2.5$, $q = 0.04$; (*b*) $M_1 = 2.5$, $q = 0.08$; (*c*) $M_1 = 2.5$, $q = 0.16$; (*d*) $M_1 = 2.5$, $q = 0.24$; (*e*) $M_1 = 3.5$, $q = 0.04$; (*f*) $M_1 = 3.5$, $q = 0.08$; (*g*) $M_1 = 3.5$, $q = 0.16$; and (*h*) $M_1 = 3.5$, $q = 0.24$.

5*b*), which supports the concept shown in figure 2(*b*). The velocity components v and w present important information regarding velocity fluctuations at the centreline of the supersonic flow. The magnitude of the fluctuations is related to the intensity of the flow instability downstream. Although the occurrence of vortex breakdown cannot be explained by flow instability, the local flow structure after the breakdown is dominated by low azimuthal wavenumbers according to a stability analysis (Garg & Leibovich 1979; Delery 1994; Meliga, Gallaire & Chomaz 2012; Qadri, Mistry & Juniper 2013; Hiejima 2017). For the cases with vortex breakdown for $q = 0.08$ (figures 4*c* and 5*c*), the fluctuation amplitudes are large around the position where the breakdown occurred

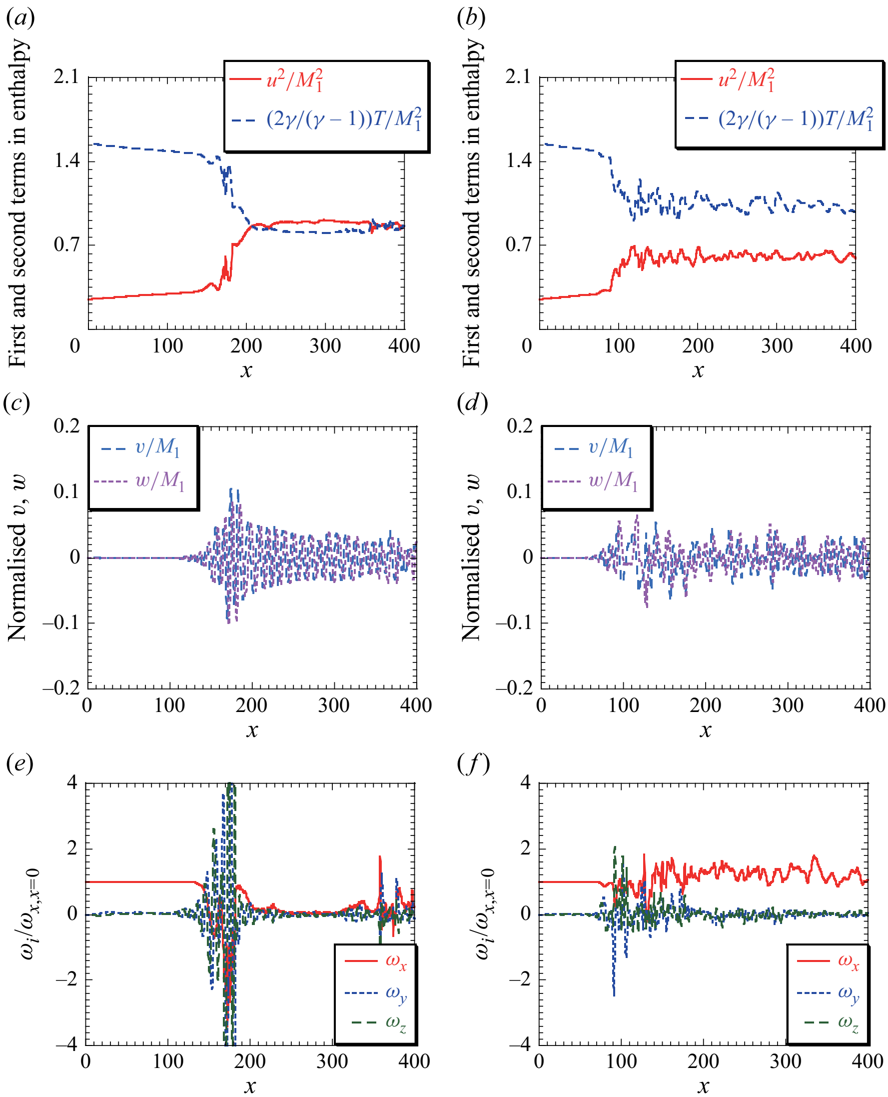

Figure 4. Streamwise variations in (*a*, *b*) normalised u^2 and T for the total enthalpy in (2.1), (*c*, *d*) normalised v and w, and (*e*, *f*) normalised vorticity ω_i at the centreline for $M_1 = 2.5$; panels (*a*, *c*, *e*) correspond to vortex breakdown ($q = 0.08$), whereas panels (*b*, *d*, *f*) correspond to no vortex breakdown ($q = 0.24$).

and convective instability appears at low wavenumbers. For the cases without vortex breakdown for $q = 0.24$ (figures 4*d* and 5*d*), the fluctuation amplitudes are small near the position where the transition occurred and only weak fluctuations occur downstream. A correlation between the absolute/convection transition and vortex breakdown is suggested (Loiseleux, Chomaz & Huerre 1998). For a Batchelor vortex in an incompressible flow, the axisymmetric mode never becomes absolutely unstable, which implies that a bubble vortex breakdown never occurs (Delbende, Chomaz & Huerre 1998). This result agrees with previous results for vortex breakdowns in supersonic flows (Hiejima 2018). An absolute instability may be specific to bubble vortex breakdown events. In addition, the axial vorticity ω_x disappears and other vorticities ω_y and ω_z occur at the centreline with a vortex breakdown (figures 4*e* and 5*e*) while ω_x is maintained downstream without a vortex

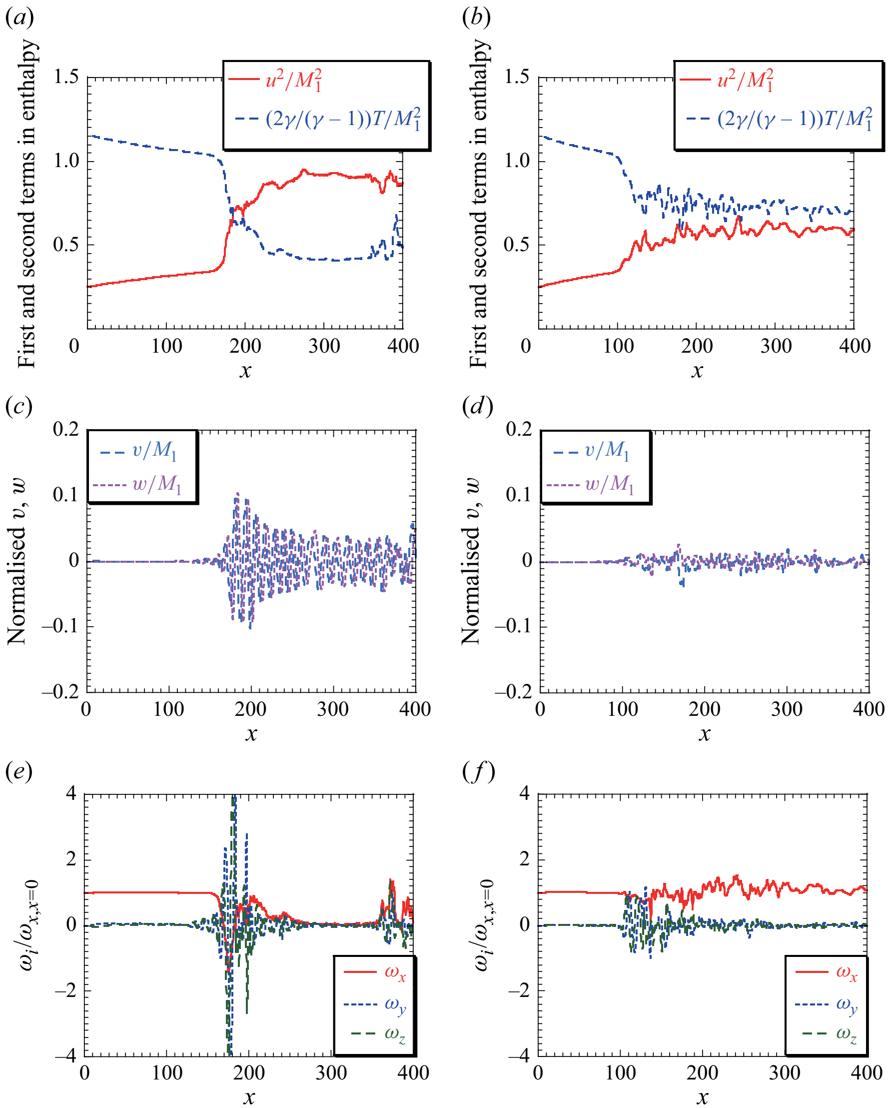

Figure 5. Streamwise variations in (a, b) normalised u^2 and T for the total enthalpy in (2.1), (c, d) normalised v and w, and (e, f) normalised vorticity ω_i at the centreline for $M_1 = 3.5$; panels (a, c, e) correspond to vortex breakdown ($q = 0.08$), whereas panels (b, d, f) correspond to no vortex breakdown ($q = 0.24$).

breakdown (figures 4f and 5f). The appearance of vorticities ω_y and ω_z is attributed to the spiral structures around the onset of vortex breakdown; then, the spiral vortex axis deviates from the centreline, and the two vorticities lead to zero at the centreline. Incidentally, judging from figure 4(a), if M_1 became smaller, (2.13) would not be satisfied. Considering that the upstream Mach number at the centreline is 1.25 for $M_1 = 2.5$, if a subsonic region exists in the flow, the condition for vortex breakdown might be close to an incompressible onset condition.

Figures 6(a) and 6(c) demonstrate that the normalised total enthalpy $\mathscr{H}_t/M_1^2$ of a supersonic flow is conserved with or without vortex breakdown. Thus, the simulation results confirm a major premise of (2.13). As mentioned in § 3, the helicity density is useful

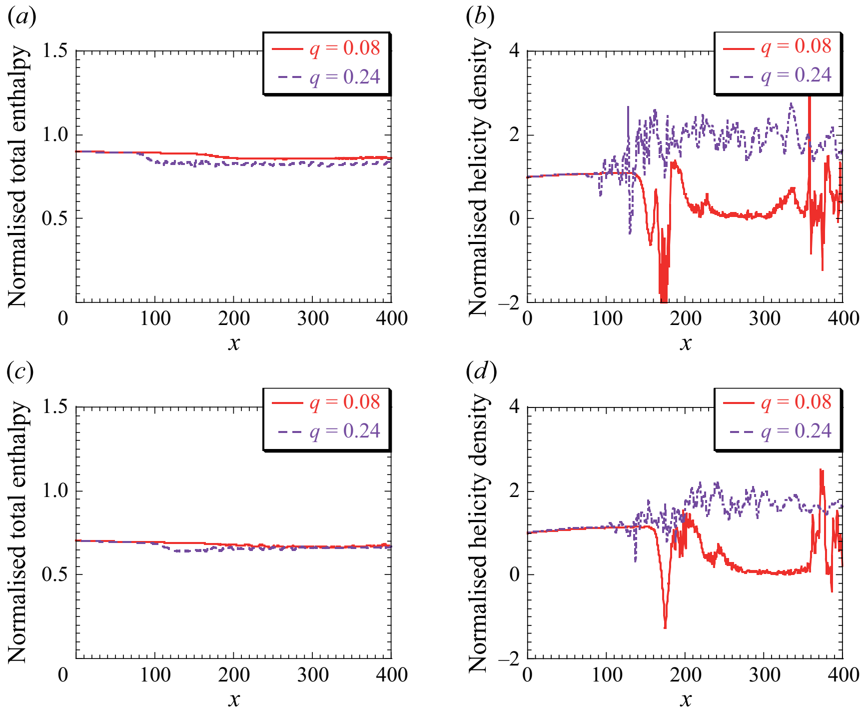

Figure 6. (*a*, *c*) Normalised total enthalpy $\mathscr{H}_t/M_1^2$ and (*b*, *d*) helicity density $h/h_{x=0}$ distributions for $q = 0.08$ and 0.24 at (*a*, *b*) $M_1 = 2.5$ and (*c*, *d*) $M_1 = 3.5$.

for evaluating the onset of vortex breakdown. In a bubble-type vortex breakdown, the streamwise velocity u is key because $\partial u/\partial x < 0$ can lead to the formation of a stagnation point. In a spiral-type vortex breakdown, ω_x disappears at the centreline; this is crucial for vortex breakdown. Hence, h includes both u and ω_x, even when v and w are not small compared with u. Figures 6(*b*) and 6(*d*) show the relationship between the helicity and vortex breakdown, where h is normalised to $h_{x=0}$. With vortex breakdown, the local helicity decreases substantially and converges to zero at the centreline. Without vortex breakdown, the helicity increases at the centreline; hence, the vortex is strengthened by circulation.

The helicity with vortex breakdown is expressed by the helicity density (3.1). By considering $\partial \omega_k/\partial x_k = 0$, (3.1) is rewritten as follows:

$$\frac{Dh}{Dt} = \underbrace{-h\frac{\partial u}{\partial x}}_{\mathrm{I}} \underbrace{-h\left(\frac{\partial v}{\partial y} + \frac{\partial w}{\partial z}\right)}_{\mathrm{II}}$$

$$\underbrace{-\omega_x\frac{\partial}{\partial x}\left(T - \frac{1}{2}u_k u_k\right)}_{\mathrm{III}} \underbrace{-\omega_y\frac{\partial}{\partial y}\left(T - \frac{1}{2}u_k u_k\right) - \omega_z\frac{\partial}{\partial z}\left(T - \frac{1}{2}u_k u_k\right)}_{\mathrm{IV}}. \tag{5.1}$$

Figure 7 plots the terms I–IV and the right-hand side of (5.1). When $q = 0.08$, the right-hand side shown in figure 7(*a*) exhibits $Dh/Dt < 0$ in most of the region. Then, term III is the most effective for $Dh/Dt < 0$, and ω_x, T and $u^2/2$ contribute significantly to

https://doi.org/10.1017/jfm.2026.11349 Published online by Cambridge University Press

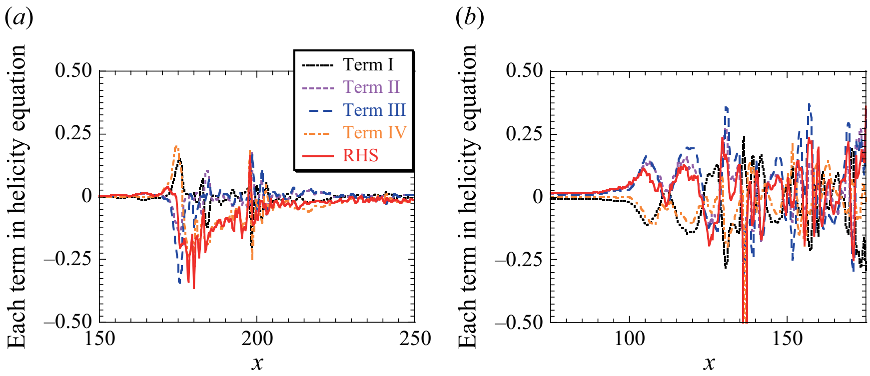

Figure 7. Terms I–IV and the right-hand side of the helicity density (5.1) at $M_1 = 3.5$: (*a*) $q = 0.08$ and (*b*) $q = 0.24$.

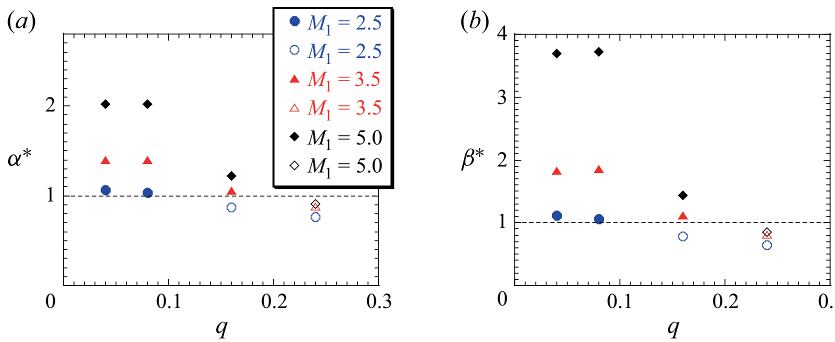

Figure 8. Comparison of the theoretical thresholds (*a*) α^* and (*b*) β^* given in (2.17) for spiral vortex breakdown and the values obtained from 3-D numerical simulations at $M_1 = 2.5$ (circle), 3.5 (triangle) and 5.0 (diamond). The filled and open symbols represent vortex breakdown and no vortex breakdown, respectively.

changes in the helicity. This is an important characteristic when vortex breakdown occurs. When $q = 0.24$, the right-hand side shown in figure 7(*b*) exhibits $Dh/Dt > 0$ after the transition.

Figure 8 shows the numerical simulation results for various q values using (2.17). These results were obtained from the physical properties after the transition, which were averaged at the centreline using the time-averaged numerical results. The filled and open symbols represent vortex breakdown and no vortex breakdown, respectively. Note that when $M_1 = 5.0$ and $q = 0.04$, the simulation was conducted in $0 \leqslant x \leqslant 600$ because the transition was inadequate in $x \leqslant 400$. According to (2.14), β^* coincides with α^*, which results in

$$\frac{J_2}{p_2} = \gamma M_2^2 + 1 > \frac{3\gamma - 1}{\gamma - 1},$$

$$M_2^2 > \frac{2}{\gamma - 1}. \tag{5.2}$$

The results in the figure are distinctly divided by the threshold in (2.17). When the longitudinal axis is more than unity, spiral vortex breakdown occurs, which is consistent with the visualisation in figure 3. Notably, the breakdown for the cases with $q = 0.16$ can be determined by the threshold. A spiral vortex breakdown also occurs when q is small, which suggests that such a vortex breakdown can occur on a delta wing at a high Reynolds number (Nelson & Pelletier 2003). Therefore, the inequality in (2.17) is a sufficient condition for determining the occurrence of spiral vortex breakdown. For mechanisms that may inhibit vortex breakdown, swirl intensity emerges as a key control parameter, as illustrated in figure 8. At sufficiently high swirl numbers, higher wavenumber modes are found to be the most unstable in the present vortex flow, whereas lower wavenumber modes commonly associated with vortex breakdown are less likely to be excited. From this perspective, local stability properties may be closely linked to the necessary conditions for the onset of vortex breakdown.

6. Conclusions

Little is known about vortex breakdowns in supersonic flows. In general, a vortex breakdown is considered as a transition between two conjugate flow states (Benjamin 1962; Mager 1972; Escudier 1988), which implies that the variation in physical variables at the centreline can be used to identify vortex breakdowns. In this study, a simple threshold (2.17) for the occurrence of spiral vortex breakdowns in supersonic flows was derived from the difference between the kinetic and internal energies based on the conservation of total enthalpy at the centreline under complete supersonic inflow conditions. (Hence, the conservation of the total enthalpy is essential for the threshold.) The numerical simulation results indicated that the occurrence of vortex breakdown reasonably satisfies the theoretical threshold. In addition, a rapid reduction in helicity was shown to be clearly related to u^2 and T in the event of a spiral vortex breakdown. This reduction in helicity provides strong evidence of the existence of a spiral vortex breakdown. This study is the first to discover this relationship and thus contributes to the understanding of vortex breakdowns in supersonic flows.

Note that this threshold is satisfied in the entire supersonic inflow region, including an axial-velocity-deficit region. In transonic and weak compressible flows near a sonic flow, a sufficient condition for the breakdown to occur would become more closely related to that of incompressible vortex breakdown. Since this problem should not be fully investigated in such regions with subsonic flow, it remains a fascinating future challenge.

Acknowledgements. This work was partly achieved through the use of large-scale computer systems SQUID at D3 Centre, Osaka University. The author expresses his deep gratitude to the anonymous referees for helping to improve the paper.

Funding. This work was supported by JSPS KAKENHI Grant Numbers JP21K11922.

Declaration of interests. The authors report no conflict of interest.

References

Althaus, W., Krause, E., Hofhaus, J. & Weiner, M. 1995 Bubble-and spiral-type breakdown of slender vortices. *Exp. Therm. Fluid Sci.* **11** (3), 276–284.

Anderson, J.D. 2003 *Modern Compressible Flow: With Historical Perspective*, 3rd edn. McGraw-Hill Education.

Batchelor, G.K. 1964 Axial flow in trailing line vortices. *J. Fluid Mech.* **20**, 645–658.

Benjamin, T.B. 1962 Theory of the vortex breakdown phenomenon. *J. Fluid Mech.* **14** (4), 593–629.

Boutros, D.W. & Gibbon, J.D. 2025 On the removal of the barotropic condition in helicity studies of the compressible Euler and ideal compressible magnetohydrodynamic equations. *J. Fluid Mech.* **1008**, R3.

Brown, G.L. & Lopez, J.M. 1990 Axisymmetric vortex breakdown part 2. Physical mechanisms. *J. Fluid Mech.* **221**, 553–576.

CATTAFESTA, L.N. & SETTLES, G.S. 1992 Experiments on shock/vortex interaction. *AIAA Paper* No. 92-0315.
DARMOFAL, D.L. 1994 A study of the mechanisms of axisymmetric vortex breakdown. PhD thesis, Massachusetts Institute of Technology.
DELBENDE, I., CHOMAZ, J.-M. & HUERRE, P. 1998 Absolute/convective instabilities in the Batchelor vortex: a numerical study of the linear impulse response. *J. Fluid Mech.* **355**, 229–254.
DELERY, J.M. 1994 Aspects of vortex breakdown. *Prog. Aerosp. Sci.* **30**, 1–59.
ESCUDIER, M. 1988 Vortex breakdown: observations and explanations. *Prog. Aerosp. Sci.* **25** (2), 189–229.
GALLAIRE, F., RUITH, M., MEIBURG, E., CHOMAZ, J.-M. & HUERRE, P. 2006 Spiral vortex breakdown as a global mode. *J. Fluid Mech.* **549**, 71–80.
GARG, A.K. & LEIBOVICH, S. 1979 Spectral characteristics of vortex breakdown flowfields. *Phys. Fluids* **22** (11), 2053–2064.
HALL, M.G. 1972 Vortex breakdown. *Ann. Rev. Fluid Mech.* **4**, 195–218.
HIEJIMA, T. 2014 Criterion for vortex breakdown on shock wave and streamwise vortex interactions. *Phys. Rev. E* **89**, 053017.
HIEJIMA, T. 2017 Streamwise vortex breakdown in supersonic flows. *Phys. Fluids* **29**, 054102.
HIEJIMA, T. 2018 Onset conditions for vortex breakdown in supersonic flows. *J. Fluid Mech.* **840**, R1.
HIEJIMA, T. 2019 Compressibility effects of supersonic Batchelor vortices. *Phys. Rev. Fluids* **4**, 093903.
HIEJIMA, T. 2020 Helicity effects on inviscid instability in Batchelor vortices. *J. Fluid Mech.* **897**, A37.
HIEJIMA, T. 2023 Streamwise vortex breakdown due to the interaction with crossed shock waves. *J. Fluid Mech.* **973**, A41.
IWABAYASHI, N., MATSUSHITA, K., OKADA, S. & HIEJIMA, T. 2024 Shock-induced supersonic combustion with a streamwise vortex. *Phys. Fluids* **36** (3), 036117.
JEONG, J. & HUSSAIN, F. 1995 On the identification of a vortex. *J. Fluid Mech.* **285**, 69–94.
KALKHORAN, I.M. & SMART, M.K. 2000 Aspects of shock wave-induced vortex breakdown. *Prog. Aerosp. Sci.* **36** (1), 63–95.
KELLER, J.J. 1994 On the practical application of vortex breakdown theory to axially symmetrical and three-dimensional compressible flows. *Phys. Fluids* **6** (4), 1515–1523.
LAMBOURNE, N.C. & BRYER, D.W. 1961 The bursting of leading-edge vortices – some observations and discussion of the phenomenon. *Aero. Res. Counc. R & M* 3282.
LEIBOVICH, S. 1978 The structure of vortex breakdown. *Ann. Rev. Fluid Mech.* **10**, 221–246.
LOISELEUX, T., CHOMAZ, J.M. & HUERRE, P. 1998 The effect of swirl on jets and wakes: linear instability of the Rankine vortex with axial flow. *Phys. Fluids* **10** (5), 1120–1134.
LUCCA-NEGRO, O. & O'DOHERTY, T. 2001 Vortex breakdown: a review. *Prog. Energy Combust. Sci.* **27**, 431–481.
MAGER, A. 1972 Dissipation and breakdown of a wing-tip vortex. *J. Fluid Mech.* **55** (4), 609–628.
MAHESH, K. 1996 A model for the onset of breakdown in an axisymmetric compressible vortex. *Phys. Fluids* **8** (12), 3338–3345.
MELIGA, P., GALLAIRE, F. & CHOMAZ, J.-M. 2012 A weakly nonlinear mechanism for mode selection in swirling jets. *J. Fluid Mech.* **699**, 216–262.
MOFFATT, H.K. & TSINOBER, A. 1992 Helicity in laminar and turbulent flow. *Ann. Rev. Fluid Mech.* **24** (1), 281–312.
NELSON, R.C. & PELLETIER, A. 2003 The unsteady aerodynamics of slender wings and aircraft undergoing large amplitude maneuvers. *Prog. Aerosp. Sci.* **39** (2), 185–248.
NOVAK, F. & SARPKAYA, T. 2000 Turbulent vortex breakdown at high Reynolds numbers. *AIAA J.* **38** (5), 825–834.
PECKHAM, D.H. & ATKINSON, S.A. 1957 Preliminary results of low speed wind tunnel tests on a gothic wing of aspect ratio 1.0. ARC. *Tech. Rep.* 508.
QADRI, U.A., MISTRY, D. & JUNIPER, M.P. 2013 Structural sensitivity of spiral vortex breakdown. *J. Fluid Mech.* **720**, 558–581.
RUITH, M.R., CHEN, P., MEIBURG, E. & MAXWORTHY, T. 2003 Three-dimensional vortex breakdown in swirling jets and wakes: direct numerical simulation. *J. Fluid Mech.* **486**, 331–378.
RUSAK, Z. & LEE, J.H. 2002 The effect of compressibility on the critical swirl of vortex flows in a pipe. *J. Fluid Mech.* **461**, 301–319.
SARPKAYA, T. 1971 On stationary and travelling vortex breakdowns. *J. Fluid Mech.* **45** (3), 545–559.
SHARMA, M. & SAMEEN, A. 2020 On the correlation between vortex breakdown bubble and planar helicity in Vogel–Escudier flow. *J. Fluid Mech.* **888**, A6.
SPALL, R. & GATSKI, T. 1990 A computational study of the taxonomy of vortex breakdown. *AIAA Paper* **1990**, 90–1624.

SPALL, R.E., GATSKI, T.B. & GROSCH, C.E. 1987 A criterion for vortex breakdown. *Phys. Fluids* **30** (11), 3434–3440.

VAN DYKE, M. 1982 *An Album of Fluid Motion*. Parabolic Press Stanford.

WEI, F., YANG, R., LIU, W.-D., ZHAO, Y.-X., WANG, Q.-C. & SUN, M. 2022 Flow structures of strong interaction between an oblique shock wave and a supersonic streamwise vortex. *Phys. Fluids* **34** (10), 106102.